Chapter 8
Advances in Prostate Cancer Imaging

Ali Aria Razmaria, Heiko Schoder, and Michael J. Morris

Introduction

The imaging of prostate cancer at different disease states has undergone a series of quantum leaps in the past decade. Imaging in prostate cancer serves, in part, the purpose of staging and risk-stratifying patients to formulate the most effective treatment plan with the least adverse side effects. However, traditional imaging techniques could only serve this role with significant limitations. Computed tomography (CT), for instance, has a size criterion of 1 cm for lymph nodes as threshold of raising suspicion for malignancy, which would not detect sub-centimeter or microscopic nodal disease often encountered on pathologic specimens. Traditional Tc-99 m methylene diphosphonate (MDP) bone scan limited by inherent single photon emission scintigraphic spatial resolution in the 1 cm range would fall short of delineating early bone metastases. Magnetic resonance imaging (MRI), despite its exquisite soft tissue resolution, faces challenges in identifying malignant lymph nodes in sub-centimeter range. To compensate for the shortcomings of standard imaging, statistical tools such as nomograms function as decision support in patient management in prostate cancer. Nomograms offer predictions based on population statistics to an individual on the risk of extraprostatic disease at diagnosis, the risk of relapse after primary therapy, or the risk of developing metastatic disease at biochemical relapse.

However, contemporary molecular imaging modalities can now more accurately depict a patient's distribution of disease on an individual level. This additional insight can supplement information from predictive models to better tailor treatment plans to an individual patient's cancer and can translate into superior treatment

A. A. Razmaria (✉) · H. Schoder · M. J. Morris
Memorial Sloan Kettering Cancer Center, New York, NY, USA
e-mail: razmaria@mskcc.org; morrism@mskcc.org

© The Author(s), under exclusive license to Springer Nature Switzerland AG 2022

K. L. Stratton, A. K. Morgans (eds.), *Urologic Oncology*,
https://doi.org/10.1007/978-3-030-89891-5_8

plans based on a more accurate understanding of a patient's disease. Tailored treatment plans can be devised by detailed knowledge of the disease characteristics and its distribution. The new paradigm of molecular imaging allows for detection of disease at a molecular level, at a stage where often no macroscopic structural abnormalities can be demonstrated. It holds the promise of answering questions not sufficiently addressed by conventional imaging and better characterizes prostate cancer at its different stages. New methods have been successfully deployed to validate these new imaging modalities and establish reference standards for comparison.

This chapter introduces different positron emission tomography (PET) imaging probes in use for prostate cancer and their mechanisms of action. Subsequently, by way of following the clinical state model of prostate cancer, we will appraise data supporting the use of different imaging modalities in each disease state, addressing challenges in clinical trial design in each instance. An emphasis will be put on PET imaging techniques with molecular imaging principles.

PET Imaging Techniques for Prostate Cancer

F-18 Sodium Fluoride PET/CT or PET/MRI Bone Scan (F-18 NaF PET Bone Scan)

The F-18-NaF PET bone scan has a mechanism of action similar to the MDP bone scan: chemisorption to hydroxyl apatite crystals in the extracellular matrix, as an indicator of osteoblastic bone turnover in response to metastatic lesions [1]. As a result, it is not the cancer but the osteoblastic activity of the bone surrounding the cancer that is imaged.

As compared to the planar single photon emission tomographic method used in the MDP bone scan, positron emission tomographic (PET) technology combined with companion low-dose CT or MRI offers better spatial resolution and immediate anatomic correlation. F-18-NaF PET/CT has superior diagnostic performance characteristics compared to a conventional MDP bone scans [2]. In addition to diagnostic advantages, F-18 NaF PET bone scan offers more patient convenience with faster study completion time (1 hour vs. typically 3 hours with an MDP bone scan), comparable radiation exposure, and only moderately increased cost [3]. However, the US Centers for Medicare and Medicaid Services does not cover this modality at the current time [4, 5].

F-18 Fluorodeoxyglucose (FDG) PET

FDG is the most commonly used PET tracer in oncology. FDG is a glucose analog and is transferred by cell membrane glucose transporters (GLUT) into the cell, where it is phosphorylated by hexokinase and trapped [6]. Many cancers have

upregulated glycolytic metabolism with overexpression of glucose transporters. While early states of prostate cancer predominantly rely on non-glycolytic metabolism (and FDG is therefore not suitable for disease staging or characterization), advanced states of the disease and high-grade tumors exhibit increased glucose metabolism [7, 8]. In the latter scenario FDG has a potential role as a prognostic biomarker and indicator of response to therapy [9–12].

C-11 Choline or F-18-Choline PET

Choline, a major component of cell membrane phospholipids, is internalized into the cell by choline transporters and metabolized by choline kinase, an enzyme overexpressed in several malignancies including prostate cancer [13–15]. The C11 isotope has a short half-life of 20 minutes, requiring on-site cyclotron production, whereas F-18, with a half-life of 110 minutes, offers logistical advantages like central radiopharmacy production and distribution. Otherwise, both tracers have similar imaging characteristics and detection rates [16]. Variable degrees of physiologic radiotracer activity in bone marrow and urinary tract, including the bladder, may interfere with the detection of early bone, pelvic nodal, and prostatic bed recurrent disease. Additional delayed post-void images may mitigate diagnostic limitations in the pelvis.

F-18 Fluciclovine

F-18 fluciclovine (anti-1-amino-3-F-18-fluorocyclobutane-1-carboxylic acid, also known as anti-F-18-FACBC) is a radiolabeled synthetic amino acid PET tracer (a leucine analog) used for the imaging of upregulated amino acid metabolism in tumors including prostate cancer [17, 18]. The tracer enters the cell by amino acid transporters including alanine, serine, cysteine transporter 2 (ASCT2), and L-type amino acid transporter 1 (LAT1), with the latter being overexpressed in high-grade prostate cancer [19, 20]. F-18 fluciclovine is not metabolized once inside the cell and can leave the cell through the same transporters. In order to optimize distribution and also because of rapid influx and efflux of the tracer into and out of prostate cancer cells, imaging must start within 3–5 minutes of the injection of radiotracer [21–23].

The advantage of low urinary excretion makes this tracer desirable for prostate cancer imaging and constitutes an advantage over other available PET tracers. A disadvantage, however, is the relatively high skeletal, muscle, and bone marrow uptake [24]. The latter can interfere with detection of osseous metastases. In addition, prostate cancer cannot be ruled out in sclerotic bone lesions seen only on CT without radiotracer activity, since dense osteoblastic lesions may lack increased F-18 fluciclovine uptake [25].

Ga-68 or F-18 Prostate-Specific Membrane Antigen (PSMA)

Prostate-specific membrane antigen (PSMA) is a transmembrane protein highly expressed on benign prostatic tissue and overexpressed by 100–1000-fold in malignant prostate epithelial cells. The PSMA gene was cloned in the research laboratory of Dr. Warren Heston at Memorial Sloan Kettering Cancer Center in 1993 [26–28]. Unlike prostate-specific antigen (PSA), which is truly prostate specific, other normal tissues like the brush border epithelium of the duodenum and small intestine, renal proximal tubule epithelium, salivary glands, as well as ganglions in nervous system also express PSMA [29–30]. Several other cancers express PSMA, including urothelial cancer of bladder, neo-vasculature of clear cell renal cancer, or endometrial cancer, albeit to a lesser extent than prostate cancer [30–34]. PSMA is a type 2 transmembrane glycoprotein enzyme involved in folate metabolism and is also known as folate hydrolase 1 [35, 36]. In the nervous system, PSMA increases the excitatory neurotransmitter glutamate and is also referred to as glutamate carboxypeptidase II (GCPII) [37]. PSMA activity in peripheral ganglionic tissue may pose a pitfall in interpretation of clinical scans. It is hypothesized that overexpression of this enzyme in malignancies may provide a growth advantage in low folate environments; other proposed functions are involvement in signal transduction and cell migration [38, 39].

The extent of PSMA overexpression in prostate adenocarcinoma correlates with Gleason grade [40, 41]. PSMA is also overexpressed in castration-resistant prostate cancer; cell lines with decreasing androgen sensitivity demonstrate increasing levels of PSMA expression [42]. Androgen-receptor-mediated signaling and PSMA expression are interconnected, and there is an inverse relationship between androgen levels and PSMA gene expression in experimental models [43, 44]. Preclinical studies demonstrate that androgen deprivation therapy (ADT) induces an increase in PSMA expression, although the ultimate effect of androgen deprivation is shrinkage in cell size and apoptosis [43]. Small-sized clinical studies appear to confirm the preclinical data with the difference that in castration-sensitive prostate cancer the rapid involutory effect of ADT appears to outweigh the initial increase in PSMA expression with the net effect of decreased detectability of lesions on PSMA scans [45]. Conversely, castration-resistant prostate cancer may display a more sustained PSMA overexpression or "PSMA flare" at further androgen manipulation with second-generation antiandrogens [46, 45]. However, larger studies in more defined prostate cancer phenotypes are required to confirm these initial observations.

Initial attempts to image prostate cancer using PSMA targeted the intracellular epitope (7E11) with indium-111-conjugated monoclonal antibodies (indium-111 capromab pendetide, ProstaScint ®). This tracer found only limited use due to multiple factors, including the difficulty of the large antibody conjugate reaching the intracellular epitope, which is only exposed in necrotic cells with membrane disruption, as well as its suboptimal imaging properties.

The desired sensitivity and specificity for imaging was subsequently achieved with the development of monoclonal antibodies and especially small molecule

ligands to the extracellular domain, particularly the active catalytic site of PSMA [36]. Among monoclonal antibodies, J591 has been most investigated in clinical trials showing good tumor localization [47]. In general, imaging with monoclonal antibodies poses several potential disadvantages, however. First, antibodies have a relatively long circulation time, resulting in a low signal-to-noise ratio due to delayed blood clearance and nonspecific background activity. The delayed blood clearance requires longer times after injection of radiotracer before imaging can be performed with an acceptable signal-to-noise ratio. These properties imply that antibodies must be tagged with longer-lived isotopes, and patients must return typically 3–5 days after the injection for the actual imaging. Available isotopes with long half-lives such as zirconium-89 (Zr-89; physical half-life 78.4 hours) meet this need, but the logistical inconvenience to patients of a multiday study remains. An additional theoretical disadvantage pertains to tumor penetration by the relatively large-sized antibody protein. Use of antibody fragments (like single-chain fragments) might be a possible solution for both challenges [48, 49].

Among several clinically introduced PSMA-targeting small molecule compounds, Ga-68 PSMA–N,N′-bis-[2-hydroxy-5-(carboxyethyl)benzyl]ethylenediamine-N,N′-diacetic acid (68Ga-HBED-CC) also known as Ga-68 PSMA 11 is probably the best studied and most widely clinically used radiotracer (Fig. 8.1). Also, a robust body of literature exists for fluorine-18-conjugated PSMA compounds N-[N-[(S)-1,3-dicarboxypropyl]carbamoyl]-4-18F-fluorobenzyl-l-cysteine, also

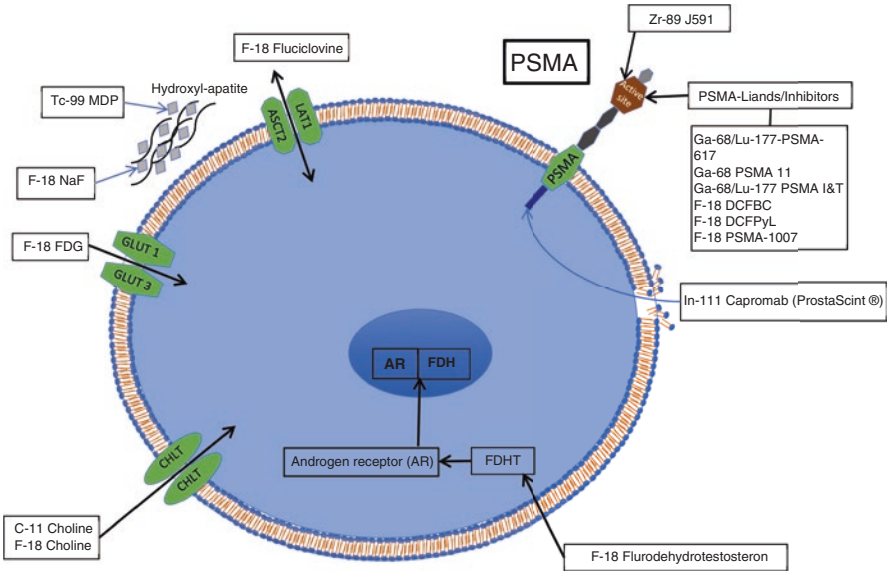

Fig. 8.1 Radiotracer distribution and targets at cellular level. *PSMA* Prostate-specific membrane antigen, *CHLT* Choline transporter, *FDG* Fluorodeoxyglucose, *GLUT* Glucose transporter, *NaF* Sodium fluoride, *MDP* Methylene diphosphonate, *ASCT2* Alanine, serine, cysteine transporter 2, *LAT1* L-type amino acid transporter 1

known as F-18 DCFBC, and the newer iteration 2-(3-[1-carboxy-5-[(6-fluoro-pyridine-3-carbonyl)-amino]-pentyl]-ureido)-pentanedioic, also known as F-18 DCFPyL [50–53]. Ga-68 PSMA 11 and F-18 DCFPyL appear to have similar imaging characteristics and share the mode of urinary excretion posing challenges in the detection of cancer in prostate fossa and in the vicinity of the bladder or ureters. Some centers utilize additional postvoid pelvic images with or without use of a diuretic to mitigate sometimes-faced diagnostic difficulties in the pelvis. Newer PSMA ligands without urinary excretion like F-18 PSMA-1007 or rh-PSMA-7 are promising, but limited data is available on these compounds at the current time [54, 55].

Although PSMA-11 has strong chelating properties for Ga-68, it does not bind the therapeutic radionuclides lutetium-177 (Lu-177) or yittrium-90 (Y-90) with the same stability. Other PSMA ligands including PSMA-671 or PSMA I&T [56] provide more stable binding for the therapeutic radionuclides. The PSMA-617 ligand can be conjugated with Ga-68 for imaging and with Lu-177 for therapy and is the agent used in recent randomized therapeutic clinical trials [57–59]. PSMA-617 features reduced kidney uptake when compared to PSMA-11, which might be of benefit in the therapeutic scenario; however, it also features urinary mode of excretion with slightly slower tracer kinetics than PSMA-11, rendering it less favorable for imaging [60]. PSMA I&T can also be conjugated with Ga-68 and with Lu-177 and demonstrates reduced hepatic uptake, but has lower lesion binding and higher background activity than PSMA-11 with the same mode of urinary excretion [61].

F-18 Fluorodehydrotestosterone PET (F-18 FDHT PET)

Investigational use of F-18 FDHT PET has also garnered special interest in the setting of advanced metastatic prostate cancer. Androgen receptor (AR) signaling plays a crucial role in the development and progression of metastatic prostate cancer. AR expression can be assessed noninvasively by F-18 FDHT, which is an analog of dihydrotestosterone (DHT) [62, 63]. Since FDHT is an analog of endogenous DHT, there is competitive binding between the two molecules for AR, similar to the relation between FDG and high levels of plasma glucose in FDG PET/CT. Therefore, this agent is used in the androgen-deprived or castrate state to obtain good target binding of the tracer. F-18 FDHT enters the cell by passive diffusion through the cell membrane because of its lipophilic properties and combines with AR in cytoplasm before translocating to the nucleus. Of note, treatment with androgen receptor blockers such as apalutamide, bicalutamide, or enzalutamide should be avoided to prevent interference with F-18 FDHT binding to AR [64]. F-18 FDHT has not yet been approved by the FDA for routine clinical use.

A cell-level depiction of distribution and targets of different tracers used in prostate cancer imaging can be found in Fig. 8.1.

Localized Disease/Initial Staging

The difficulty of imaging prostate cancer is in part explained by its often-multifocal presentation on histology within the prostate gland and confounding factors including commonly present benign prostatic hyperplasia or prostatitis. This is why an initial diagnosis is, in many cases, established by systematic sampling of the entire prostate gland as opposed to targeted biopsy of a suspicious lesion, as is the case in many other malignancies. The clinical questions in localized prostate cancer pertain to the presence of unifocal versus multifocal disease, extracapsular extension, seminal vesicle invasion, and neurovascular bundle involvement. In cases of nomogram-predicted high probability of metastasis (intermediate- and high-risk disease), evaluation for metastatic sites, including nodal and osseous disease, becomes relevant at initial staging. The presence of metastatic disease has direct implications for treatment planning and can change the approach from localized treatment to systemic therapy or a combination of both.

The paucity of high-quality data in this realm is in part explained by challenges in trial design, which apply to imaging trials at all stages of prostate cancer but are most tangible in the setting of localized disease. Patients diagnosed with prostate cancer with low risk of metastasis based on elevated PSA who subsequently obtained standard systematic biopsy will undergo radical prostatectomy and template pelvic nodal dissection. Consequently, proposed new imaging modalities in this setting will always be compared to histology as gold standard. As a result, an imaging tool with a technical resolution limit in millimeter range will be compared to microscopy with resolution in micrometer range. Hence, the diagnostic performance of macroscopic imaging modalities invariably suffers in sensitivity; historically, for many clinicians, this has implied a lack of utility. Clinics are increasingly adopting the perspective that not all prostate cancers require treatment and not each microscopic focus is clinically relevant, sparking renewed interest in distinguishing specifically clinically relevant disease. The implementation of new outcome measures in imaging trials — such as the detection of dominant focus of disease, high-grade disease, specificity, or correct localization — has opened new avenues in imaging trial design. Although new molecular imaging probes narrow the gap between macroscopic and microscopic disease, and molecular tracers can overcome size constraints by high levels of target expression, the resolution boundaries of imaging instrumentation and hardware remain a limitation.

Magnetic Resonance Imaging (MRI)

Multiparametric MRI (mpMRI) has changed the imaging landscape of localized prostate cancer by improving on the detection rates of high-grade tumors offered by ultrasound or computed tomography (CT). Due to its high soft tissue resolution,

MRI can also delineate locally advanced disease with relative accuracy, with a sensitivity and specificity for extraprostatic extension of 49% and 82% and for seminal vesicle involvement of 45% and 96% [65, 66]. This anatomical characterization can inform subsequent treatment planning.

In a retrospective study of 150 prostate cancer patients, investigators evaluated the detection of clinically significant prostate cancer (Gleason score ≥4 + 3) by mpMRI and correlated imaging findings with whole mount pathology mapping from subsequent prostatectomy. Using the Prostate Imaging Reporting and Data System version 2 (PI-RADSv2), 94% (118/125) of peripheral zone and 95% (42/44) of transition zone tumors with a tumor volume equal or greater than 0.5 mL were detected. However, only 26% (7/27) of peripheral zone and 20% (2/10) of transition zone tumors with a Gleason score ≥4 + 3, but less than 0.5 mL tumor volume, were identified, pointing out the limited sensitivity in small-volume intermediate- to high-grade lesions [67]. As a result of data like these and others [68], prostate biopsies are increasingly performed based on MRI or as MRI-guided biopsies, in addition to systematic sampling of the prostate. At the current time mpMRI remains the imaging standard of choice for detection and localization of tumor within prostate gland and assessment of extracapsular extension or seminal vesicle involvement.

PET Imaging Probes

Limited data exists evaluating the application of PET agents for intra-gland localization of prostate cancer. Furthermore, many PET agents show similar uptake in prostate cancer, benign prostatic hyperplasia, and prostatitis reducing the ability to localize disease within the prostate. Nevertheless, preliminary data combining newer PET imaging agents with pelvic MRI for primary tumor localization (T-staging) suggest a beneficial effect in diagnostic performance. In a small prospective study of 21 men with prostate cancer, serial 3 Tesla mpMRI of the prostate and F-18 fluciclovine PET/CT within 6-month interval were obtained to evaluate for localization of cancer within prostate. All patients underwent radical prostatectomy for histological confirmation. When all tumors where included, sensitivities and specificities of 67% and 66%, for F-18 fluciclovine PET/CT, and 73% and 79%, for MRI, respectively, were demonstrated. When localization of dominant tumors was assessed, both imaging modalities achieved 90% sensitivity. The combination of both modalities yielded a positive predictive value (PPV) of 82% for localization of any tumor within prostate, a value higher than each modality separately [69].

One can compellingly argue that the most important component of staging is not detection of disease in the prostate, which will be done by biopsy, but the detection of extraglandular disease. For most patients, the pelvic nodes represent the boundary between locoregional and systemic disease and the potential for cure rather than chronic management. Hence, PET imaging has extensively been explored for the purposes of initial staging, with a particular toward assessing the status of the pelvic nodes. There is some prospective evidence for metabolic PET probes like choline

(C-11 or F-18) or F-18 fluciclovine in the setting of initial staging of intermediate- to high-risk prostate cancer. In a prospective study of 210 patients with intermediate- to high-risk prostate cancer, Poulsen et al. evaluated the presence of nodal metastases at initial staging using F-18 choline with histological confirmation by pelvic node dissection. A sensitivity of 73.2% and specificity of 87.6% in per-patient nodal staging was demonstrated. Incidental bone lesions in 18 patients, consistent with metastases, not detected on standard bone scintigraphy, were noted. No central scan reporting or measure of inter-reader agreement was included [70].

Beheshti et al. evaluated F-18 choline PET in a prospective cohort of 130 patients with intermediate- to high-risk prostate cancer. With pathologic confirmation in 111 (85%) patients, a per-patient nodal staging sensitivity and specificity of 45% and 96%, respectively, was found. Interestingly, for lymph node metastases of 5 mm or larger in diameter, an improved sensitivity of 66% (unchanged specificity) was shown. Incidental detection of occult bone metastases in 13 patients was also reported. No central independent reporting or blinding to clinical history of readers was incorporated in the study design [71].

Using F-18 fluciclovine PET/MRI for preoperative lymph node staging in high-risk prostate cancer, Selnaes et al. prospectively evaluated a small cohort of 28 patients and compared findings of PET and MR images, interpreted by separate readers, using 3 Tesla MRI as scan equipment and the mpMRI protocol to assess the prostate. An extended pelvic lymph node dissection was carried out in 26 patients, who comprised the final study cohort. Patient-based sensitivity/specificity for detection of pelvic lymph node metastases was 40%/87.5% for MRI and 40%/100% for F-18 fluciclovine, respectively [72]. No independent central reporting or measure of inter-reader agreement was employed. Although small in size, this study suggests a higher specificity for F-18 fluciclovine than MRI at a similar sensitivity.

Finally, in a meta-analysis of both C-11 and F-18 choline PET, Evangelista et al. evaluated ten studies, the majority of which were prospective small- to moderate-sized cohorts (12–130 patients) including the study by Beheshti et al. (overall 441 patients). In the setting of initial staging of intermediate- to high-risk prostate cancer and employing histological confirmation, a pooled sensitivity of 49% and pooled specificity of 95% was reported [73].

More robust, regulatory-quality contemporary data is available on PET agents that target the prostate-specific membrane antigen (PSMA) for initial staging. The FDA approved Ga-68 PSMA-11 PET in December 2020 and F-18 DCFPyl in May 2021, multiplying the options for FDA-approved agents in the setting of initial staging of prostate cancer with increased risk for metastasis [74, 75]. Both PSMA PET agents appear to have similar imaging characteristics with direct comparisons between the two agents currently lacking. A summary of select studies with emphasis on pivotal trials leading to regulatory approvals of PET agents for initial staging of prostate cancer is provided in Table 8.1.

In the OSPREY study, a prospective multicenter trial, Pienta et al. evaluated the diagnostic performance with sensitivity and specificity as co-primary endpoints of F-18 DCFPyL PET in 252 patients with high-risk prostate cancer undergoing radical prostatectomy with pelvic lymphadenectomy (cohort A). In a separate cohort B,

Table 8.1 Summary of selected studies with emphasis on trials leading to FDA approval of PET agents in initial staging of high-risk prostate cancer

	Total patients	PSA (ng/mL)	Primary endpoint	Central read	Sensitivity (SE) Specificity (SP)	Histopathologic confirmation	Nodal tumor size
Ga-68 PSMA 11							
Hope et al. 2020 [77]	633	Median (range) 11.1 (0.04–147)	SE/SP Detection of PLNM	Yes	SE 40% SP 95%	277 patients (44%)	Average 10 mm in TP Average 4 mm in FN
F-18 DCFPyL							
Osprey, Pienta et al. 2021 [76]	268	Median (range) 9.7 (1.2–125.3)	SE/SP Detection of PLNM	Yes	SE 40.3% SP 97.9%	252 patients (94%)	For >5 mm SE 60% SP 97.9%
F-18 Choline							
Beheshti et al. 2010 [71]	130	Range 0.25–462	SE/SP Detection of PLNM	No	SE 45% SP 96%	111 patients (85%)	For ≥5 mm SE 66% SP 97.9%
3 Tesla MRI							
von Below et al. 2016 [68]	40	Range 10–20	SE/SP Detection of PLNM	No	SE 55% SP 90%	40 patients (100%)	Average 12.3 mm in TP Average 5.2 mm in FN

FN False negative, *TP* True positive, *SE* Sensitivity, *SP* Specificity, *PSMA* Prostate-specific membrane antigen, *PLNM* Pelvic nodal metastasis, *PET* Positron emission tomography

93 evaluable prostate cancer patients with suspected recurrence or metastases on conventional imaging undergoing biopsies were enrolled. Central independent reporting of scans with blinding to clinical information was obtained and measures of inter-reader and intra-reader agreement provided. In cohort A, a median specificity of 97.9% and median sensitivity of 40.3% (the latter not meeting the prespecified endpoint for sensitivity) was reported. In a post hoc sensitivity analysis of cohort A, exploring detection of nodal metastases larger than 5 mm, assuming that smaller tumor foci are below PET detection limits, resulted in a sensitivity of 60%

(unchanged high specificity), meeting the prespecified confidence bounds for sensitivity. For cohort B, the median sensitivity and PPV for extraprostatic lesions were 95.8% and 81.9%, respectively. F-18 DCFPyL PET, although similar in sensitivity to conventional imaging, including CT and MRI, demonstrated consistently higher specificity and PPVs in the setting of initial staging of high-risk prostate cancer [76].

Similarly, Hope et al. evaluated the sensitivity and specificity of Ga-68 PSMA PET for nodal detection in a prospective multicenter cohort of 633 patients with intermediate- to high-risk prostate cancer. Scans were read by independent central readers blinded to clinical information. A majority rule was applied for final consensus interpretation. With histopathologic confirmation by way of pelvic nodal dissection in 277 patients (44%), a per-patient sensitivity of 40% and specificity of 95% were demonstrated. Also in this trial, the size of nodal involvement was associated with detectability with an average node size of 10 mm in true-positive patients as compared to 4 mm in false-negative patients [77].

In the proPSMA trial, a prospective multicenter randomized study with crossover design, authors investigated the accuracy of Ga-68 PSMA PET as first-line imaging compared to CT and bone scan for detection of pelvic nodal and distant metastases in patients with high-risk prostate cancer. Patients either underwent curative-intent surgery or radiotherapy. A predefined reference standard including histopathology, imaging, and biochemistry at 6-month follow-up was applied. Scans were reported by central independent readers in addition to local readers, and high measures of inter-reader agreement were reported. Of 339 assessed patients for eligibility, 302 men were randomly assigned equally to the two study arms. Patients crossed over unless three or more distant metastases were identified. Of 295 (98%) men with follow-up, 87 (30%) had pelvic nodal or distant metastatic disease. Conventional imaging including CT and bone scan had lower sensitivity (38% vs. 85%) and lower specificity (91% vs. 98%) compared with PSMA PET-CT. In addition, management changes occurred more frequently with PSMA PET as compared to conventional imaging (28% vs. 15%), and PSMA PET conveyed less equivocal findings than conventional imaging (7% vs. 23%). Furthermore, in patients with second-line imaging following crossover, more management changes ensued after second-line PSMA PET versus second-line conventional imaging in 27% versus 5%, respectively. The authors concluded that PSMA PET is a suitable replacement for combined CT and bone scan in initial staging of high-risk prostate cancer [78].

The proPSMA trial provided compelling high-quality evidence that PSMA PET can replace bone scan and CT in the initial staging of high-risk prostate cancer and can be considered practice-changing. However, the initial T-staging of high-risk prostate cancer will continue to rely on mpMRI, due to the shortcomings of currently available PSMA PET agents in the evaluation of the prostate gland, which relate in part to urine PSMA excretion and normal mild PSMA expression in prostatic tissue.

Biochemical Recurrent (BCR) Prostate Cancer

Biochemical recurrence follows initial definitive treatment with curative intent, either with radical prostatectomy or radiation therapy. This crucial disease state represents recurrence without radiographic evidence of disease by standard techniques. Biochemical recurrence is defined as when prostate-specific antigen (PSA) values rise above 0.2 ng/mL after radical prostatectomy or rise 2 ng/mL or more above the nadir PSA following definitive radiation therapy of the prostate (ASTRO Phoenix consensus definition) [79]. About 20–40% of patients after radical prostatectomy [80–82] and 30–50% after radiation therapy [83] develop biochemical recurrence 10 years after treatment. The importance of this disease state and interest in more accurate imaging modalities rests on the assumption that early accurate detection of recurrent disease constitutes a window of opportunity for curative or "salvage" treatment. For instance, the RADICALS-RT randomized prospective phase III trial, comparing adjuvant radiation therapy versus salvage radiation in 1396 men after prostatectomy with high-risk features for progression (i.e., pT3/4 disease, Gleason score 7–10, positive margins, or preoperative PSA level >10 ng/mL), supported early salvage radiation therapy over adjuvant radiation [84]. The results of this trial further increased the interest of clinicians in better characterization of recurrent disease at low PSA values.

While the patterns of recurrence are variable, some clinicopathological characteristics can help predict sites of recurrent disease which in turn can guide treatment decisions. For example, in patients with positive surgical margins after radical prostatectomy, local recurrence is more common [85]. On the other hand, biochemical recurrence within 6 months of radical prostatectomy, short PSA doubling time, and unsurprisingly nodal involvement on pathology are predictors of metastasis [86–88].

Historically, patients with BCR underwent imaging with abdominopelvic computed tomography and bone scan. However, these imaging modalities have limited sensitivity. For instance, a standard bone scan is positive for metastatic disease in less than 5% of cases if the PSA value is below 7 ng/mL in the biochemical recurrence setting [89–91]. Similarly, CT studies in men experiencing BCR after surgery with a mean PSA value in the range of 2.4–33.1 ng/mL detect disease in only 11–14% of patients [92, 93].

One conundrum in clinical trial design in this setting in developing new imaging modalities is the establishment of a reference standard or gold standard. Often, the ideal scenario of obtaining histological confirmation in lesions detected by imaging is not feasible or possible due to small size, location, multiplicity, or patient preference. In such situations, many well-designed studies establish a composite reference of "truth" based on subsequent imaging or PSA response to targeted therapy. As in the setting of initial staging of prostate cancer, the utility of F-18 FDG PET and F-18 NaF PET is not well established in the biochemical recurrence setting and has not been tested in well-designed prospective trials.

In the following section, FDA-approved PET agents in the biochemical recurrent setting will be discussed.

C-11 Choline or F-18 Choline PET

In the setting of BCR prostate cancer after radical prostatectomy or radiation therapy, the US Food and Drug Administration (FDA) approved in 2012 the use of C-11 choline PET after noninformative conventional imaging.

In a retrospective study of 176 patients with biochemical recurrence and a median PSA of 7.2 ng/mL, investigators evaluated the detection of recurrent disease by C-11 choline PET. Patients had undergone either a radical prostatectomy, radiation therapy, or cryoablation as initial treatment. Studies were reported as clinical reads by local readers with access to clinical information and prior imaging. No measures of inter-reader agreement were investigated. Histological confirmation was obtained in 73 patients (41%) with conventional imaging (CT, bone scan, and MRI) serving as confirmation in remaining cases. A per-patient sensitivity of 93%, specificity of 76%, PPV of 91%, and an overall detection rate of 75% (132/176) were reported. Sites of detection were in the pelvic lymph nodes (68 of 132, 51.5%), prostatectomy bed (38 of 132, 38.8%), skeleton (26 of 132, 19.7%), mediastinum (3 of 132, 2.3%), and prostate (14 of 132, 10.6%). Detection rates based on PSA value were 31% at less than 0.5 ng/mL, 56% for 0.5–1.0 ng/mL, 68% for 1.1–2.0 ng/mL, 84% for 2.1–5.0 ng/mL, and 89% above 5 ng/mL. The value of 2 ng/mL was proposed as the best cutoff to distinguish a positive scan from a negative scan with a probability value of 0.73. Findings on C-11 choline PET were deemed clinically useful and lead to a management change in 56% [94].

In a retrospective cohort of 358 patients with biochemical recurrence (mean PSA 3.77 ng/mL) after radical prostatectomy, the diagnostic performance of C-11 choline and detection rates for C-11 choline at different PSA values were studied. PET/CT findings were validated using histological criteria in 13% (46/358) of patients and follow-up clinical and imaging criteria in 87% (312/358). Scans were interpreted by local readers independently with knowledge of clinical history and consensus resolutions of discrepancies. An interobserver agreement of 94% was reported. Sensitivity, specificity, PPV, negative predictive value, and overall accuracy were 85%, 93%, 91%, 87%, and 89%, respectively. Overall detection rate was 45% (161/358) with detection rate per anatomical region of 66% in lymph nodes, 34% in prostatectomy bed, and 29% in skeleton [95]. Detection rates correlated with PSA value, with 13% in PSA equal or less than 0.6 ng/ml, 29% for 0.6–1 ng/mL, 46% for 1–2 ng/mL, 60% for 2–5 ng/mL, and 83% above 5 ng/mL.

In a more contemporary retrospective cohort of 287 patients with biochemical recurrence (median PSA 0.94 ng/mL) after surgery or radiotherapy, investigators used C-11 choline PET for localization of recurrent disease. Two local readers, one blinded to clinical information and one unblinded, reported separately on each study utilizing a 3-point scale (0 = negative, 1 = equivocal, 2 = positive), with a consensus read constituting the final designation. Intra-reader and inter-reader concordance were 86% and 76%, respectively. When scores 1 and 2 were considered positive, an overall detection rate of 66% was found, and PSA level detection rates of 45% for less than 0.5 ng/mL, 56% for 0.5–0.99 ng/mL, 70% for 1.0–1.99 ng/mL, and 90%

for equal or greater than 2.0 ng/mL were obtained. Considering only scores of 2 as positive, the overall detection rate was 54%, and PSA cutoff detection rates were of 28%, 46%, 62%, and 81%, PSA less than 0.5 ng/mL, 0.5–0.99 ng/mL, 1.0–1.99 ng/mL, and equal or greater than 2.0 ng/mL, respectively, were reported. In the final consensus read, 47 (16.4%) scans were equivocal. Histological confirmation was obtained in 49 patients (17%). Patterns of recurrence were overall 20.3% in the prostate bed, 48% in the pelvic nodes, 5.6% in the extrapelvic lymph nodes, 10.5% in bone, and 1.4% in visceral metastases (17.8% extrapelvic metastases). Recurrent sites outside the initial treatment field were observed in 28% of patients [96].

A meta-analysis of 18 in majority retrospective studies including two of studies mentioned above, with a total of 2126 patients, demonstrated a pooled detection rate of 62% and a pooled sensitivity and specificity of 89% and 89%, respectively [97]. The studies varied in inclusion of patients after radical prostatectomy, radiation therapy, or both as well as in PSA value at time of imaging with a mean and median PSA ranging from 0.9 ng/ml to 21.1 ng/ml and 0.5 ng/ml to 10.7 ng/ml, respectively. Reporting of scans varied across studies and some studies used readers blinded to clinical history to interpret results. All studies used a composite reference standard including histology (in average 26%), other imaging (CT, MRI, and bone scan), and clinical follow-up for more than 12 months, including repeated imaging after treatment. Pooled detection rates among studies were 27% for local recurrence, 36% for nodal metastasis, and 25% for bone metastasis.

F-18 Fluciclovine

The diagnostic performance of F-18 fluciclovine in comparison to In-111 capromab pendetide was evaluated in a prospective single-center cohort of 50 patients with BCR (mean PSA 6.62 ng/mL) after definitive therapy for prostate cancer including prostatectomy and radiation therapy. Studies were each interpreted by two local readers with disagreement resolved by consensus. No measures of interobserver agreement were explored. The reference standard was a combination of tissue correlation in 18% (9/50), imaging, laboratory, and clinical data. F-18 fluciclovine had a disease detection sensitivity and specificity in the prostate bed of 89% and 67% and a sensitivity of 100% and specificity of 100% in extraprostatic recurrence. F-18 fluciclovine was more sensitive than In-111 capromab pendetide SPECT/CT in the detection of recurrent prostate carcinoma [98]. One might argue that the comparison to In-111 capromab pendetide, which is FDA approved in BCR setting, is not clinically relevant.

In a multicenter retrospective study including 596 patients with BCR after initial therapy, including prostatectomy and radiation therapy, an overall detection rate of 67.7% by F-18 fluciclovine was reported [99]. Image interpretation was based on clinical reads without utilization of central blinded readers. Anatomic site-specific detection rates were 38.7% in the prostate/prostate bed, 32.6% in pelvic lymph nodes, and 26.2% for metastatic involvement outside the pelvis. The overall

detection rate based on PSA level was 41.4% in the PSA range of 0.79 ng/ml or less, approximately 60% (45% for extraprostatic disease) in the range 0.8–2.03 ng/ml, approximately 75% (45% for extraprostatic disease) in the range 2.04–6.00 ng/ml, and approximately 85% (approximately 60% for extraprostatic disease) for PSA above 6 ng/mL. Based on histological confirmation in 143 patients, a lesion-based overall PPV of 62.2% with site-specific PPV of 92.3% for extraprostatic lesions and 71.8% for prostate/prostate bed involvement was described. Patient-based sensitivity, specificity, and PPV were, 91%, 40%, and 82%. The authors associate the suboptimal specificity and PPV with confounding factors that occur when the prostate is still in place, caused by overlap of activity with prostatitis and BPH as well as, in part, sampling errors for histology. This assumption is supported by the relatively high proportion of patients after radiotherapy for prostate cancer in the cohort and discrepantly low lesion-based PPV for prostate/prostate bed lesions as compared to extraprostatic sites of disease.

In the LOCATE trial, a prospective multicenter study of 213 patients in BCR setting (median PSA 1.0 ng/mL), the authors evaluated as a primary endpoint the change in planned treatment. The study results were based on clinical reads without central readers or blinding of interpreters to clinical information. No routine histological confirmation was pursued, and diagnostic test performance was not the primary goal of the study. A detection rate of F-18 fluciclovine-avid lesions in 122 patients (57%) was reported. The detection rate was 30% in the prostate/prostate bed and 38% outside the prostate, i.e., 29% in lymph nodes, 2.3% in soft tissue, and 11% in bone.

Detection rates based on PSA values in this trial were 31% for PSA ranges of 0–0.5 ng/ml, 50% for PSA 0.5–1.0 ng/ml, 66% for PSA 1.0–2.0 ng/ml, approximately 75% for PSA 2.0–5.0 ng/mL, and approximately 87% above 5 ng/mL. A change in management after the scan was instated in 59% of patients [100].

The differences in detection rate between the different studies are explained by their different populations — e.g., radical prostatectomy patients versus patients after radiation therapy with prostate gland in situ — as well as different PSA cutoff values. A recent systematic review and meta-analysis reported a pooled sensitivity of 0.79 (95% CI 0.60–0.91) and a pooled specificity of 0.69 (95% CI 0.59–0.77) for F-18 fluciclovine for BCR prostate cancer [101].

The higher diagnostic yield by F-18 fluciclovine PET compared to conventional imaging including CT, bone scan, or MRI has repercussions in assessment of eligibility for and planning of radiation therapy (RT). The EMPIRE-1 study, a single-center, phase II/III trial, randomized 165 patients with biochemical recurrence and negative conventional imaging to either standard template-based RT versus RT informed by F-18 fluciclovine PET [102]. All patients had prior radical prostatectomy with a median PSA of 0.34 ng/mL at time of recurrence. Radiation fields included the prostate bed, with or without inclusion of pelvic lymph nodes. The primary outcome was 3-year event-free survival, defined as biochemical recurrence or progression, or initiation of systemic therapy. Four patients in the F-18 fluciclovine PET group were deemed ineligible for RT due to extrapelvic or skeletal lesions. With a median follow-up of 3.5 years, a significant difference in event-free survival

of 63.0% (95% confidence interval 49.2–74.0) in the conventional imaging group versus 75.5% (95% confidence interval 62.5–84.6) in the F-18 fluciclovine PET group (difference 12.5; 95% confidence interval 4.3–20.8; $p = 0.0028$) was observed. This study indicates that beyond improvements in diagnostic test performance, this new-generation PET agent translates into tangible clinical benefit. Similar maturing radiation therapy clinical trials evaluating PSMA-PET tracers and comparing PSMA PET to F-18 fluciclovine PET are underway and will likely better inform indication and planning of radiation therapy for BCR prostate cancer.

Ga-68 or F-18 Prostate-Specific Membrane Antigen (PSMA)

Based on FDA approval of Ga-68 PSMA-11 PET in December 2020 and F-18 DCFPyl in May 2021 also in the BCR setting, concomitant with time of compilation of this book chapter, the choices of FDA-approved agents in this disease state of prostate cancer have further expanded [74, 75]. Both PSMA PET agents appear to have also similar imaging characteristics in BCR scenario with head-to-head comparisons currently not available.

A prospective multicenter trial of Ga-68 PSMA evaluated 635 patients with biochemical recurrence (median PSA 2.1 ng/mL) after radical prostatectomy or radiation therapy with the endpoints of PPV, detection rate, and inter-reader reproducibility, using central readers with three independent reads per study and blinding of readers to clinical information or prior imaging. Lesions were validated by histopathologic analysis in 87 patients and a composite reference standard in remaining cases. An overall detection rate of 75% and site-specific detection rate of 26% in prostate bed/prostate, 38% in pelvic lymph nodes (N1 disease), 17% in extrapelvic lymph nodes or visceral organs (M1a/M1c disease), 16% in bones (M1c disease), and 7% in multiple sites (Multiple M1) were reported [103]. Overall, 35% had pelvic-only disease and 49% extrapelvic involvement. Detection rates based on PSA cutoffs were 38% for PSA values less than 0.5 ng/mL, 57% for PSA 0.5–1.0 ng/mL, 84% for PSA 1.0–2.0 ng/mL, 86% for PSA 2.0–5.0 ng/mL, and 97% for PSA values above 5.0 ng/mL. A patient-based PPV of 84% by histopathologic validation was demonstrated and 92% by composite reference standard where no histopathologic confirmation was available. Interestingly, several cases of false-positive interpretation were intraprostatic lesions after radiation therapy [103].

The CONDOR trial, a prospective multicenter study of F-18 DCFPyL PSMA PET, evaluated 208 men after primary therapy including prostatectomy and radiation therapy for prostate cancer, who were experiencing biochemical relapse (median PSA 0.8 ng/mL) without evidence of disease on conventional imaging [53]. The primary endpoint of the study was correct localization rate (CLR), a term that corresponds to PPV with the additional requirement of anatomical colocalization. This endpoint as corresponded to the F-18 DCFPyL PET-positive lesions that met the criteria of the study's composite standard of truth. The reference standard of

truth consisted of histopathology in 31 patients, correlative imaging in 100 patients, and PSA response after radiation therapy in one patient. Central independent readers blinded to clinical information as well as local readers were utilized. A CLR of 84.8–87.0% was reported. This finding translates to a 13.0–15.2% false-positive rate. Region-based PPVs were 79.5% for prostate/prostatic bed, 70.9% for pelvic lymph nodes, 67.4% for extrapelvic metastasis (M1), 61.5% for extrapelvic lymph nodes (M1a), 62.5% for bone (M1b), and 28.6% for visceral disease. The overall detection rate was 59–66% and rose with PSA values, with 36% at less than 0.5 ng/mL, 51% for 0.5–1.0 ng/mL, 67% for 1.0–2.0 ng/mL, 85% for 2.0–5.0 ng/mL, and 97% for 5.0 ng/mL and above. A change in intended management occurred in 63.9% of evaluable patients. A high inter-reader and intra-reader agreement was achieved.

There is a paucity of data comparing C-11 choline/F-18 choline, F-18 fluciclovine, and Ga-68 PSMA-11/F-18 PSMA DCFPyL in the setting of BCR prostate cancer. In a small prospective study of 50 patients with BCR after radical prostatectomy undergoing F-18 fluciclovine and C-11 choline PET scans, overall detection rates were 34% versus 22% (37 lesions vs. 23 lesions, respectively, p-value < 0.0001) [104]. Site-specific detection rates for F-18 fluciclovine and C-11 choline were 10% versus 6% for local recurrence (5 vs. 3 lesions, p-value < 0.0001), 20% versus 10% for nodal disease (15 vs. 6 lesions, p-value < 0.0001), and 10% versus 8% for bone metastasis (17 vs. 14 lesions, p-value < 0.0001), respectively. Detection rates based on PSA cutoff values were 21% versus 14% below 1 ng/mL, 20% versus 13% for 1–2 ng/mL, 33% versus 17% for 2–3 ng/mL, and 60% versus 40% above 3 ng/mL. It is hypothesized that the suggested superiority of F-18 fluciclovine over C-11 choline may have biological underpinnings. For example, in prostate cancer cell lines, fluciclovine uptake is higher than choline, acetate, or methionine uptake [105, 106].

Another small, prospective study comparing Ga-68 PSMA-11 to F-18 fluciclovine demonstrated higher detection rates with PSMA-11 PET, especially in the low PSA range. A head-to-head comparison of 50 patients experiencing biochemical recurrence after prostatectomy and with PSA range of 2 ng/mL or less demonstrated an overall detection rate of 56% for Ga-68 PSMA-11 versus 26% for F-18 fluciclovine (Odds ratio of 4.8, 95% CI 1.6–19.2; p-value = 0.0026) [107]. In the same study, site-specific detection rates of Ga-68 PSMA-11 and F-18 fluciclovine were 30% versus 8% (Odds ratio 12.0, 95% CI 1·8–513·0, p = 0·0034) for pelvic nodal disease and 16% versus 0% for any extrapelvic lesions (Odds ratio and CI non-estimable, p-value = 0·0078), respectively. Of note, detection of local recurrence in the prostate bed suggested a trend towards superior detection with F-18 fluciclovine (14% vs. 18%), although this finding remains hypothesis-generating and in need of further evaluation.

In the absence of high-quality comparative evidence, it appears prudent to combine pelvic MRI with PSMA PET (if available) for local pelvic evaluation of disease in the BCR setting. In fact, based on physiologic excretion of Ga-68 PSMA and F-18 PSMA PET agents, evaluation of local recurrence in prostatic fossa may be compromised. Furthermore, PSMA PET has limited sensitivity in detection of recurrent prostate cancer within prostate gland after radiation therapy, likely due to

false-positive PSMA activity in postradiation inflammatory prostate gland changes [103]. F-18 fluciclovine is the only approved PET agent in the BCR setting with no or limited urinary excretion and may be considered as a tracer to evaluate suspected or equivocal findings in the prostatic surgical bed.

The advent of new targeted molecular imaging tracers like PSMA that can better detect disease will serve to redefine disease states. For example, patients considered to have non-metastatic castration-resistant prostate cancer (nmCRPC) based on conventional imaging will likely be reclassified with better imaging tools, as having metastatic disease. A vivid demonstration of this stage migration was published in a retrospective review of 200 patients classified as nmCRPC based on conventional imaging at six different centers who then underwent PSMA PET imaging. Central review revealed that 196 patients had positive scans, with 55% reclassified as having M1 disease despite negative conventional imaging [108]. This stage migration has significant implications for clinical trial design in terms of defining both eligibility criteria and relapse.

Approximately 5–10% of prostate cancers do not express PSMA to a significant degree on immunohistochemistry (IHC) [109]. These cancers are as expected PSMA-PET negative [110, 111]. Furthermore, there is heterogeneity in the intensity and extent of PSMA expression in primary tumors and to a lesser degree also in lymph node metastases on IHC [112, 113]. Although prior reports show strong associations between tumor grade and PSMA expression, even high-grade and high-volume metastatic disease can be PSMA-negative [113]. There appears to be a correlation between PSMA expression in the primary tumor (or percentage of tumor negative for PSMA) and nodal metastasis, which is associated with PSMA-PET detectability [113].

An illustration of different PET tracers commonly used in biochemical settings is provided in Fig. 8.2. Table 8.2 summarizes select studies with an emphasis on pivotal trials leading to regulatory approvals of PET agents for BCR prostate cancer.

Metastatic Prostate Cancer

In the United States, 5% of patients present with a diagnosis of metastatic disease, versus 77% with localized and 11% with regional disease [114]. Approximately, 15% of patients with localized disease treated with curative intent primary therapy develop metastatic disease with most frequent sites in lymph nodes (38.2%) and bones (36.8%) [115]. In the United States, a 5-year survival for metastatic prostate cancer improved from 28.7% from 2001–2005 to 32.3% from 2011–2016 [114]. This is at least in part related to expanded effective treatment strategies.

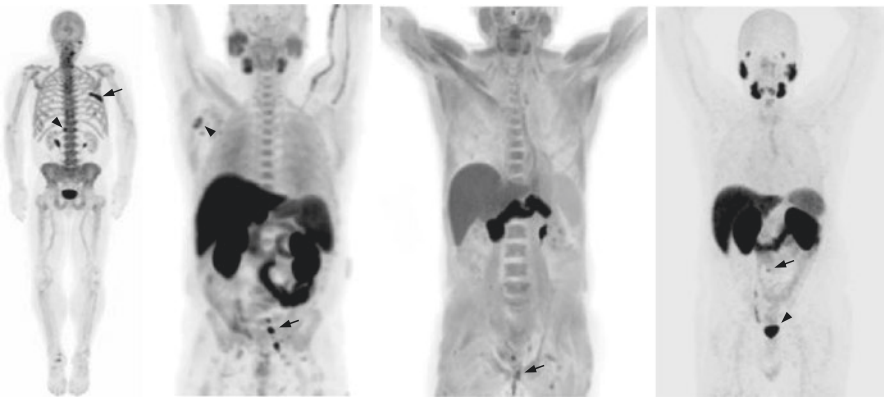

F-18 Sodium Fluoride PET/CT Bone Scan
Prostatectomy, PSA 2.0 ng/mL. Metastasis to left 7th rib (arrow). Degenerative uptake along the spine (arrowhead).

C-11 Choline PET/CT
Radiation to prostate, PSA 4.8 ng/mL. Suspicious left pelvic lymph nodes (arrow), reactive right axillary lymph nodes (arrowhead). Note normal diffuse tracer activity in bones and lack of activity in bladder.

F-18 Fluciclovine PET/CT
Prostatectomy, PSA 3.3 ng/mL, Local recurrence at bladder neck (arrow). Note normal diffuse tracer activity in bones and lack of activity in bladder.

Ga-68 PSMA PET/CT
Prostatectomy, PSA 1.4 ng/mL. Suspicious retroperitoneal lymph node (arrow). Note normal tracer activity in bladder (arrowhead).

Fig. 8.2 Use of different PET probes in biochemical recurrence prostate cancer. *PET* Positron emission tomography, *CT* Computed tomography, *PSA* Prostate-specific antigen

Treatment Response

The purpose of imaging in advanced metastatic disease is to describe the extent of disease, provide information on response to therapy, and define the etiology of clinical symptoms, such as pathologic fractures or cord compression. Cornerstones of imaging at this stage remain conventional imaging, including bone scan, CT, and MRI. Computed tomography is of value to delineate nodal disease and visceral involvement. MRI is helpful in better characterizing visceral disease with the probable exception of lung and early bone metastases. The standard MDP bone scan remains relevant in the metastatic setting and is included in the recommendations of the Prostate Cancer Clinical Trial Working Group 3 (PCWG 3) for assessment of osseous metastatic disease in clinical trials [116]. These criteria for defining radiographic progression in metastatic prostate cancer are a prospectively validated measure of progression that correlates well with overall survival and has therefore earned regulatory recognition for the purposes of new drug approval [117–119]. According to PCWG 3 recommendations, progression of osseous disease is confirmed only if two or more lesions appear on first bone scan after initiation of therapy and at least an additional two lesions are seen on the subsequent bone scan at least 6 weeks later. At later time points in the course of treatment, osseous progression is established if at least two new confirmed lesions appear relative to the first

Table 8.2 Summary of select studies with emphasis on trials leading to FDA approval of PET agents in BCR prostate cancer

	Total patients	Study design	PSA (ng/mL)	Primary outcome	Initial treatment	Central read	Detection rate (overall/ per region)	Detection Rate by PSA (ng/mL) stratification		Pathologic confirmation
F-18/C-11 choline										
Mitchell et al. 2013 [94]	176	Retro	Median (range) 7.2 (2.2–1028.0)	SE, SP, DR	RP, RT, Cryo	No	75% PR: 10.6% PB: 38.8% PLN: 51.5% Bone: 19.7% Visc: 2.3%	<0.5	31%	73 pts. (41%)
								0.5–1.0	56%	
								1.1–2.0	68%	
								2.1 to 5.0	84%	
								>5.0	89%	
Michaud et al. 2020 [96]	287	Retro	Median (range) 0.94 (0.15–89.9)	DR	RP, RT	No	66% PB: 20.3% PLN: 48%% EPLN: 5.6% Bone: 10.5% Visc: 1.4% EP: 17.8%	<0.5	45% (28%)[a]	49 pts. (17%)
								0.5–0.99	56% (46%)[a]	
								1.0–1.99	70% (62%)[a]	
								≥2.0	90% (81%)[a]	
F-18 Fluciclovine										
Schuster et al. 2011 [98]	50	Pros	Mean (range) 6.62 (0.11–44.74)	SE, SP, DR	RP, RT, Cryo, HIFU	No	PB: 74% SE: 89% SP: 67% EPD: 24% SE: 100% SP: 100%	N/A		PB: 46 pts. (92%) EPD: 9 pts. (18%)
Bach-Gansmo et al., 2017 [99]	596	Retro	Median (range) 2.0 (0.05–82.0)	DR, SE, SP, PPV	RP, RT, other	No	DR: 67.7% PR/PB: 38.7% PLN: 32.6% EP: 26.2%	≤0.79	41.4%	143 pts. (24%)
								0.8–2.03	60%	
								2.04–6.00	75%	
								>6	85%	

LOCATEAndriole et al. 2019 [100]	213	Pros	Median (range) 1.0 (0.2–93.5)	DR, change in management	RP, RT, Cryo, HIFU	No	DR: 57% PR/PB: 30% LN: 29% Bone: 11% Visc: 2.3% EPD: 38%	0–0.5 0.5–1.0 1.0–2.0 2.0–5.0 > 5	31% 50% 66% 75% 87%	N/A
Ga-68 PSMA 11										
Fendler et al. 2019 [103]	635	Pros	Median (range) 2.1 (0.1–1154)	AC	RP, RT	Yes	DR: 75% PR/PB: 26% PLN: 38% EPLN/Visc: 17% Bone: 16% Multiple sites: 38% EPD: 49%	<0.5 0.5 to <1.0 1.0 to <2.0 2.0 to <5.0 ≥5.0	38% 57% 84% 86% 97%	87 pts. (13.7%)
F-18 DCFPyL-PSMA										
CONDOR Morris et al. 2020 [131]	208	Pros	Median (range) 0.8 (0.17–98.4)	CLR, PPV	RP, RT	Yes	DR 59–66% PPV per region: PR/PB: 79.5% PLN: 70.9% EP: 67.4% EPLN: 61.5% Bone: 62.5% Visc: 28.6%	< 0.5 0.5 to <1.0 1.0 to <2.0 2.0 to <5.0 ≥5.0	36% 51% 67% 85% 97%	31 pts. (14.9%)

[a]When equivocal reads considered negative

RP Radical prostatectomy, *RT* Radiation therapy, *Cryo* Cryosurgery, *Retro* Retrospective, *Pros* Prospective, *SE* Sensitivity, *SP* Specificity, *DR* Detection rate, *CLR* Correct localization rate, *AC* Accuracy, *PPV* Positive predictive value, *PB* Prostate bed, *PR* Prostate, *PLN* Pelvic lymph nodes, *EPLN* Extrapelvic lymph nodes, *LN* Lymph nodes, *Visc* Visceral, *EP* Extrapelvic metastasis, *EPD* Extraprostatic disease, *PET* Positron emission tomography, *HIFU* High-intensity modulated ultrasound, pts. Patients, *N/A* Not available

on-treatment scan [116]. These recommendations avoid misinterpreting a flare after initiation of therapy as progression or transient benign osseous foci as disease. However, few prospective studies have examined, much less validated, a definition for response assessments for new imaging modalities.

F-18 NaF bone scan has capabilities similar to the MDP bone scan, with increased sensitivity and more precise quantification stemming from the addition of improved resolution based on PET technology. Several studies demonstrate the value of NaF-PET bone scan for quantification of osseous metastatic burden, response to therapy, and differentiation between flare phenomena and true progression in bone-only metastatic prostate cancer [120, 121]. Nonetheless, F-18 NaF is still limited to imaging bone, rather than any quality of the tumor itself.

In all likelihood, PSMA will be used to assess treatment response for metastatic disease; however, studies validating how a meaningful change on a PSMA scan manifests have yet to be performed.

Biologic Characterization

FDG-PET provides prognostic information on dedifferentiating prostate cancer with high glycolytic activity [7, 11, 12] and is frequently used at some centers in this stage of disease. It has received increasing scrutiny for its potential role in identifying aggressive cancers that may have undergone treatment-emergent lineage plasticity, which occurs as a complex adaptive process involving both genomic and epigenetic factors when prostate cancers are subjected to androgen signaling inhibition [122–126]. Preliminary studies have indicated that FDG has a role in identifying neuroendocrine prostate cancer on a lesional level [127]; even more provocatively, FDG has been combined with FDHT to directly image for the presence of androgen receptor expression with an intact ligand binding domain. In a cohort of 133 men with metastatic castration-resistant prostate cancer (mCRPC) who were naïve to androgen receptor signaling inhibitors (ARSi), Fox et al. performed serial FDG PET/CT and FDHT PET/CT scans evaluating for glycolysis and androgen receptor expression patterns with correlation to overall survival. In 2405 lesions, the following imaging phenotypes emerged: 71.2% with both FDG and FDHT avidity, 16.0% with FDHT but not FDG avidity, and 12.7% with FDG but not FDHT avidity. The latter group would be expected to have the most similarities to a population undergoing lineage plasticity, and indeed these patients had the worst prognosis of any group. The study demonstrated that the heterogeneity of the PET/CT phenotype has clinical relevance on a lesion and patient level. Most lesions expressed androgen receptors, consistent with the initial benefit of second-line ARSi drugs in the mCRPC setting. At the same time, on a patient level, 49% had at least one lesion without FDHT uptake and with FDG uptake — the imaging phenotype with the most negative effect on survival, possibly due to ARSi resistance [128]. This work must be considered preliminary, with future studies comparing imaging findings and biologic correlates.

The ability to noninvasively assess AR expression can be used as part of drug development as a pharmacodynamic marker. FDHT was indeed used in the original dose-finding studies for both enzalutamide and apalutamide to establish AR saturation and occupancy and can be used for the development of new classes of AR-degrading agents or inhibitors for pre-treatment stratification, planning of clinical trials, and response assessment [129, 130].

Theranostics

With the advent of new therapeutic avenues using PSMA-targeting radionuclide therapies, the use of molecular imaging to determine PSMA expression as part of a theranostic approach in advanced prostate cancer will grow increasingly relevant in the near future. Emerging data support the use of lutetium-177 PSMA-targeted therapy in the setting of advanced metastatic prostate cancer. In the TheraP trial, a randomized phase II multicenter trial evaluating lutetium-177 PSMA-617 (Lu-177 PSMA) versus cabazitaxel in patients with metastatic castration-resistant prostate cancer [59], 200 patients underwent Ga-68 PSMA-11 PET as well as F-18 FDG PET imaging as part of their eligibility assessment. Patients included in the study were those with PSMA-expressing disease and no sites of metastatic disease with discordant FDG-positivity and PSMA-negative findings. A case of discordant PSMA PET and FDG PET is illustrated in Fig. 8.3. PSA responses were significantly more frequent among patients in the Lu-177 PSMA arm than in the cabazitaxel arm: 65% versus 37% (66% vs. 37% by intention to treat; difference 29% [95% CI 16–42; $p < 0{\cdot}0001$; and 66% vs. 44% by treatment received; difference 23% [95% CI 9–37; $p = 0{\cdot}0016$]).

The international VISION trial, a randomized open-label phase III study evaluating Lu-177 PSMA-617 plus standard of care (SOC) in men with PSMA-positive mCRPC versus SOC alone, recently reported similarly positive outcomes with significantly improved primary endpoint of overall survival in the Lu-177 PSMA-617 group (median OS, 15.3 vs. 11.3 months; HR, 0.62 [95% CI: 0.52, 0.74]; $p < 0.001$, one-sided). The other primary endpoint, radiologic progression-free survival (rPFS), was also strongly positive, with a 60% reduction in the risk of radiographic progression or death and a 5-month improvement in time to rPFS (HR = 0.40, $p < 0.001$, median 8.7 vs. 3.4 months). These patients were selected only on the basis of Ga-68 PSMA 11 scans alone with no FDG imaging. Eighty-seven percent of the patients were allowed into the study on the basis of a positive PSMA PET scan, with only 13% screen-failing by imaging criteria. These data would suggest that FDG imaging may not be necessary to identify patients who will clinically benefit from therapeutic lutetium-based PSMA-directed radioligand therapy. Whether or not FDG further improves outcomes, or PSMA alone is sufficient, or even the relationship between either imaging modality or a treatment benefit from Lu-177 PSMA-617 is not known. These areas will all require further study. These recent therapy trials suggest that the novel radioligand therapy with Lu-177 PSMA-617 will soon enter the

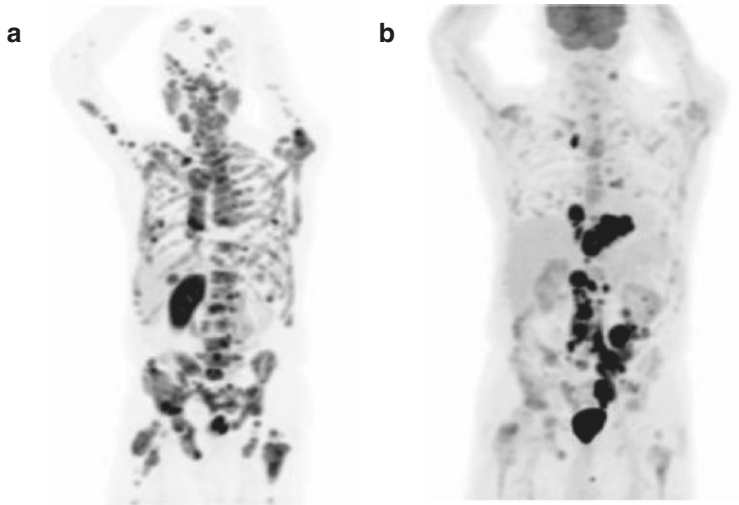

Ga-68 PSMA PET (Panel A) and FDG PET (Panel B) in a patient with metastatic castration resistant prostate Cancer (PSA 361 ng/mL) within 1-week interval. Intense PSMA activity in osseous and hepatic metastasis without significant activity in FDG avid pulmonary metastasis, thoracoabdominal adenopathy and masses encasing left upper urinary tract. Lack of tracer activity in left kidney due to obstructive nephropathy.

Fig. 8.3 Concurrent use of FDG PET and Ga-68 PSMA PET in advanced prostate cancer. *PSMA* Prostate-specific membrane antigen, *FDG* Fluorodeoxyglucose, *PET* Positron emission tomography

clinical practice for the treatment of advanced prostate cancer and that PSMA PET imaging will play a key role in determining the eligibility of patients for this treatment.

In summary, imaging of prostate cancer at its various stages is undergoing a transformation. The fight against prostate cancer will benefit broadly from molecular imaging paradigms. The abundance of available choices in imaging options, as compared to a decade ago, approaches the metaphor of a transition from famine to feast. Responsibility now lies in the hands of experienced clinicians and imaging experts to tailor the optimal imaging approach, in full awareness of strengths and shortcomings of each modality, meeting clinical need along the spectrum of disease stages in prostate cancer.

Ultimately, new imaging modalities, beyond diagnostic test performance, ideally need to demonstrate improved patient outcomes. Initial high-level evidence demonstrates the benefit in such outcomes achieved by new-generation PET imaging tools. Ongoing and future studies will potentially further substantiate the translation of better imaging characterization of prostate cancer to improved patient outcomes.

References

1. Czernin J, Satyamurthy N, Schiepers C. Molecular mechanisms of bone 18F-NaF deposition. J Nucl Med. 2010;51(12):1826–9.
2. Grant FD, Fahey FH, Packard AB, Davis RT, Alavi A, Treves ST. Skeletal PET with 18F-fluoride: applying new technology to an old tracer. J Nucl Med. 2008;49(1):68–78.
3. Mick CG, James T, Hill JD, Williams P, Perry M. Molecular imaging in oncology: (18) F-sodium fluoride PET imaging of osseous metastatic disease. AJR Am J Roentgenol. 2014;203(2):263–71.
4. Centers For Medicare & Medicaid Services. Decision Memo for Positron Emission Tomography (NaF-18) to Identify Bone Metastasis of Cancer (CAG-00065R2); 2015. Available from: https://www.cms.gov/medicare-coverage-database/details/nca-decision-memo.aspx?NCAId=279.
5. American College Of Radiology. CMS Refuses Medicare Coverage of NaF PET Scans 2018.
6. Macheda ML, Rogers S, Best JD. Molecular and cellular regulation of glucose transporter (GLUT) proteins in cancer. J Cell Physiol. 2005;202(3):654–62.
7. Jadvar H. Imaging evaluation of prostate cancer with 18F-fluorodeoxyglucose PET/CT: utility and limitations. Eur J Nucl Med Mol Imaging. 2013;40 Suppl 1:S5–10.
8. Beauregard JM, Blouin AC, Fradet V, Caron A, Fradet Y, Lemay C, et al. FDG-PET/CT for pre-operative staging and prognostic stratification of patients with high-grade prostate cancer at biopsy. Cancer Imaging. 2015;15:2.
9. Fox JJ, Morris MJ, Larson SM, Schoder H, Scher HI. Developing imaging strategies for castration resistant prostate cancer. Acta Oncol. 2011;50 Suppl 1:39–48.
10. Scher HI, Morris MJ, Larson S, Heller G. Validation and clinical utility of prostate cancer biomarkers. Nat Rev Clin Oncol. 2013;10(4):225–34.
11. Meirelles GS, Schoder H, Ravizzini GC, Gonen M, Fox JJ, Humm J, et al. Prognostic value of baseline [18F] fluorodeoxyglucose positron emission tomography and 99mTc-MDP bone scan in progressing metastatic prostate cancer. Clin Cancer Res. 2010;16(24):6093–9.
12. Fox JJ, Gavane SC, Blanc-Autran E, Nehmeh S, Gonen M, Beattie B, et al. Positron emission tomography/computed tomography-based assessments of androgen receptor expression and glycolytic activity as a prognostic biomarker for metastatic castration-resistant prostate cancer. JAMA Oncol. 2018;4(2):217–24.
13. Schoder H, Larson SM. Positron emission tomography for prostate, bladder, and renal cancer. Semin Nucl Med. 2004;34(4):274–92.
14. Michel V, Yuan Z, Ramsubir S, Bakovic M. Choline transport for phospholipid synthesis. Exp Biol Med (Maywood). 2006;231(5):490–504.
15. Ramirez de Molina A, Rodriguez-Gonzalez A, Gutierrez R, Martinez-Pineiro L, Sanchez J, Bonilla F, et al. Overexpression of choline kinase is a frequent feature in human tumor-derived cell lines and in lung, prostate, and colorectal human cancers. Biochem Biophys Res Commun. 2002;296(3):580–3.
16. von Eyben FE, Kairemo K. Meta-analysis of (11)C-choline and (18)F-choline PET/CT for management of patients with prostate cancer. Nucl Med Commun. 2014;35(3):221–30.
17. Shoup TM, Olson J, Hoffman JM, Votaw J, Eshima D, Eshima L, et al. Synthesis and evaluation of [18F]1-amino-3-fluorocyclobutane-1-carboxylic acid to image brain tumors. J Nucl Med. 1999;40(2):331–8.
18. Schuster DM, Votaw JR, Nieh PT, Yu W, Nye JA, Master V, et al. Initial experience with the radiotracer anti-1-amino-3-18F-fluorocyclobutane-1-carboxylic acid with PET/CT in prostate carcinoma. J Nucl Med. 2007;48(1):56–63.
19. Oka S, Okudaira H, Yoshida Y, Schuster DM, Goodman MM, Shirakami Y. Transport mechanisms of trans-1-amino-3-fluoro[1-(14)C]cyclobutanecarboxylic acid in prostate cancer cells. Nucl Med Biol. 2012;39(1):109–19.
20. Segawa A, Nagamori S, Kanai Y, Masawa N, Oyama T. L-type amino acid transporter 1 expression is highly correlated with Gleason score in prostate cancer. Mol Clin Oncol. 2013;1(2):274–80.

21. Gusman M, Aminsharifi JA, Peacock JG, Anderson SB, Clemenshaw MN, Banks KP. Review of (18)F-Fluciclovine PET for detection of recurrent prostate cancer. Radiographics. 2019;39(3):822–41.
22. Blue Earth Diagnostics. Axumin prescription information; 2016. Available from: https://www.axumin.com/sites/default/files/2018-03/Axumin_PI_08_2016_Clean.pdf.
23. Nanni C, Zanoni L, Bach-Gansmo T, Minn H, Willoch F, Bogsrud TV, et al. [(18)F]Fluciclovine PET/CT: joint EANM and SNMMI procedure guideline for prostate cancer imaging-version 1.0. Eur J Nucl Med Mol Imaging. 2020;47(3):579–91.
24. Schuster DM, Nanni C, Fanti S, Oka S, Okudaira H, Inoue Y, et al. Anti-1-amino-3-18F--fluorocyclobutane-1-carboxylic acid: physiologic uptake patterns, incidental findings, and variants that may simulate disease. J Nucl Med. 2014;55(12):1986–92.
25. Lowentritt BH, Kipper MS. Understanding and improving (18)F-Fluciclovine PET/CT reports: a guide for physicians treating patients with biochemical recurrence of prostate cancer. Prostate Cancer. 2020;2020:1929565.
26. Israeli RS, Powell CT, Fair WR, Heston WD. Molecular cloning of a complementary DNA encoding a prostate-specific membrane antigen. Cancer Res. 1993;53(2):227–30.
27. Israeli RS, Powell CT, Corr JG, Fair WR, Heston WD. Expression of the prostate-specific membrane antigen. Cancer Res. 1994;54(7):1807–11.
28. O'Keefe DS, Bacich DJ, Huang SS, Heston WDW. A perspective on the evolving story of PSMA biology, PSMA-based imaging, and endoradiotherapeutic strategies. J Nucl Med. 2018;59(7):1007–13.
29. Ristau BT, O'Keefe DS, Bacich DJ. The prostate-specific membrane antigen: lessons and current clinical implications from 20 years of research. Urol Oncol. 2014;32(3):272–9.
30. Mhawech-Fauceglia P, Zhang S, Terracciano L, Sauter G, Chadhuri A, Herrmann FR, et al. Prostate-specific membrane antigen (PSMA) protein expression in normal and neoplastic tissues and its sensitivity and specificity in prostate adenocarcinoma: an immunohistochemical study using mutiple tumour tissue microarray technique. Histopathology. 2007;50(4):472–83.
31. Silver DA, Pellicer I, Fair WR, Heston WD, Cordon-Cardo C. Prostate-specific membrane antigen expression in normal and malignant human tissues. Clin Cancer Res. 1997;3(1):81–5.
32. Thorek DL, Watson PA, Lee SG, Ku AT, Bournazos S, Braun K, et al. Internalization of secreted antigen-targeted antibodies by the neonatal Fc receptor for precision imaging of the androgen receptor axis. Sci Transl Med. 2016;8(367):367ra167.
33. Kinoshita Y, Kuratsukuri K, Landas S, Imaida K, Rovito PM Jr, Wang CY, et al. Expression of prostate-specific membrane antigen in normal and malignant human tissues. World J Surg. 2006;30(4):628–36.
34. Samplaski MK, Heston W, Elson P, Magi-Galluzzi C, Hansel DE. Folate hydrolase (prostate-specific membrane [corrected] antigen) 1 expression in bladder cancer subtypes and associated tumor neovasculature. Mod Pathol. 2011;24(11):1521–9.
35. Pinto JT, Suffoletto BP, Berzin TM, Qiao CH, Lin S, Tong WP, et al. Prostate-specific membrane antigen: a novel folate hydrolase in human prostatic carcinoma cells. Clin Cancer Res. 1996;2(9):1445–51.
36. Maurer T, Eiber M, Schwaiger M, Gschwend JE. Current use of PSMA-PET in prostate cancer management. Nat Rev Urol. 2016;13(4):226–35.
37. Hlouchova K, Barinka C, Klusak V, Sacha P, Mlcochova P, Majer P, et al. Biochemical characterization of human glutamate carboxypeptidase III. J Neurochem. 2007;101(3):682–96.
38. Ghosh A, Heston WD. Tumor target prostate specific membrane antigen (PSMA) and its regulation in prostate cancer. J Cell Biochem. 2004;91(3):528–39.
39. Rajasekaran AK, Anilkumar G, Christiansen JJ. Is prostate-specific membrane antigen a multifunctional protein? Am J Physiol Cell Physiol. 2005;288(5):C975–81.
40. Bostwick DG, Pacelli A, Blute M, Roche P, Murphy GP. Prostate specific membrane antigen expression in prostatic intraepithelial neoplasia and adenocarcinoma: a study of 184 cases. Cancer. 1998;82(11):2256–61.

41. Marchal C, Redondo M, Padilla M, Caballero J, Rodrigo I, Garcia J, et al. Expression of prostate specific membrane antigen (PSMA) in prostatic adenocarcinoma and prostatic intraepithelial neoplasia. Histol Histopathol. 2004;19(3):715–8.
42. Denmeade SR, Sokoll LJ, Dalrymple S, Rosen DM, Gady AM, Bruzek D, et al. Dissociation between androgen responsiveness for malignant growth vs. expression of prostate specific differentiation markers PSA, hK2, and PSMA in human prostate cancer models. Prostate. 2003;54(4):249–57.
43. Evans MJ, Smith-Jones PM, Wongvipat J, Navarro V, Kim S, Bander NH, et al. Noninvasive measurement of androgen receptor signaling with a positron-emitting radiopharmaceutical that targets prostate-specific membrane antigen. Proc Natl Acad Sci U S A. 2011;108(23):9578–82.
44. Bakht MK, Oh SW, Youn H, Cheon GJ, Kwak C, Kang KW. Influence of androgen deprivation therapy on the uptake of PSMA-targeted agents: emerging opportunities and challenges. Nucl Med Mol Imaging. 2017;51(3):202–11.
45. Emmett L, Yin C, Crumbaker M, Hruby G, Kneebone A, Epstein R, et al. Rapid modulation of PSMA expression by androgen deprivation: serial (68)Ga-PSMA-11 PET in men with hormone-sensitive and castrate-resistant prostate cancer commencing androgen blockade. J Nucl Med. 2019;60(7):950–4.
46. Ettala O, Malaspina S, Tuokkola T, Luoto P, Loyttyniemi E, Bostrom PJ, et al. Prospective study on the effect of short-term androgen deprivation therapy on PSMA uptake evaluated with (68)Ga-PSMA-11 PET/MRI in men with treatment-naive prostate cancer. Eur J Nucl Med Mol Imaging. 2020;47(3):665–73.
47. Tagawa ST, Beltran H, Vallabhajosula S, Goldsmith SJ, Osborne J, Matulich D, et al. Anti-prostate-specific membrane antigen-based radioimmunotherapy for prostate cancer. Cancer. 2010;116(4 Suppl):1075–83.
48. Holland JP, Divilov V, Bander NH, Smith-Jones PM, Larson SM, Lewis JS. 89Zr-DFO-J591 for immunoPET of prostate-specific membrane antigen expression in vivo. J Nucl Med. 2010;51(8):1293–300.
49. Wiehr S, Buhler P, Gierschner D, Wolf P, Rolle AM, Kesenheimer C, et al. Pharmacokinetics and PET imaging properties of two recombinant anti-PSMA antibody fragments in comparison to their parental antibody. Prostate. 2014;74(7):743–55.
50. Cho SY, Gage KL, Mease RC, Senthamizhchelvan S, Holt DP, Jeffrey-Kwanisai A, et al. Biodistribution, tumor detection, and radiation dosimetry of 18F-DCFBC, a low-molecular-weight inhibitor of prostate-specific membrane antigen, in patients with metastatic prostate cancer. J Nucl Med. 2012;53(12):1883–91.
51. Chen Y, Pullambhatla M, Foss CA, Byun Y, Nimmagadda S, Senthamizhchelvan S, et al. 2-(3-{1-Carboxy-5-[(6-[18F]fluoro-pyridine-3-carbonyl)-amino]-pentyl}-ureido)-pen tanedioic acid, [18F]DCFPyL, a PSMA-based PET imaging agent for prostate cancer. Clin Cancer Res. 2011;17(24):7645–53.
52. Rowe SP, Macura KJ, Mena E, Blackford AL, Nadal R, Antonarakis ES, et al. PSMA-based [(18)F]DCFPyL PET/CT is superior to conventional imaging for lesion detection in patients with metastatic prostate cancer. Mol Imaging Biol. 2016;18(3):411–9.
53. Morris MJ, Rowe SP, Gorin MA, Saperstein L, Pouliot F, Josephson DY, et al. Diagnostic performance of (18)F-DCFPyL-PET/CT in men with biochemically recurrent prostate cancer: results from the CONDOR phase 3, multicenter study. Clin Cancer Res. 2021.
54. Kuten J, Fahoum I, Savin Z, Shamni O, Gitstein G, Hershkovitz D, et al. Head-to-head comparison of (68)Ga-PSMA-11 with (18)F-PSMA-1007 PET/CT in staging prostate cancer using histopathology and immunohistochemical analysis as a reference standard. J Nucl Med. 2020;61(4):527–32.
55. Eiber M, Kroenke M, Wurzer A, Ulbrich L, Jooss L, Maurer T, et al. (18)F-rhPSMA-7 PET for the detection of biochemical recurrence of prostate cancer after radical prostatectomy. J Nucl Med. 2020;61(5):696–701.
56. Weineisen M, Schottelius M, Simecek J, Baum RP, Yildiz A, Beykan S, et al. 68Ga- and 177Lu-labeled PSMA I&T: optimization of a PSMA-targeted theranostic concept and first proof-of-concept human studies. J Nucl Med. 2015;56(8):1169–76.

57. Afshar-Oromieh A, Hetzheim H, Kratochwil C, Benesova M, Eder M, Neels OC, et al. The theranostic PSMA ligand PSMA-617 in the diagnosis of prostate cancer by PET/CT: biodistribution in humans, radiation dosimetry, and first evaluation of tumor lesions. J Nucl Med. 2015;56(11):1697–705.
58. Morris M. Phase III study of lutetium-177-PSMA-617 in patients with metastatic castration-resistant prostate cancer (VISION). J Clin Oncol, 2021;39:(suppl 15; abstr LBA4) 2021. Available from: https://meetinglibrary.asco.org/record/196661/abstract.
59. Hofman MS, Emmett L, Sandhu S, Iravani A, Joshua AM, Goh JC, et al. [(177) Lu]Lu-PSMA-617 versus cabazitaxel in patients with metastatic castration-resistant prostate cancer (TheraP): a randomised, open-label, phase 2 trial. Lancet. 2021.
60. Farolfi A, Calderoni L, Mattana F, Mei R, Telo S, Fanti S, et al. Current and emerging clinical applications of PSMA PET diagnostic imaging for prostate cancer. J Nucl Med. 2021;62(5):596–604.
61. Herrmann K, Bluemel C, Weineisen M, Schottelius M, Wester HJ, Czernin J, et al. Biodistribution and radiation dosimetry for a probe targeting prostate-specific membrane antigen for imaging and therapy. J Nucl Med. 2015;56(6):855–61.
62. Liu A, Dence CS, Welch MJ, Katzenellenbogen JA. Fluorine-18-labeled androgens: radiochemical synthesis and tissue distribution studies on six fluorine-substituted androgens, potential imaging agents for prostatic cancer. J Nucl Med. 1992;33(5):724–34.
63. Larson SM, Morris M, Gunther I, Beattie B, Humm JL, Akhurst TA, et al. Tumor localization of 16beta-18F-fluoro-5alpha-dihydrotestosterone versus 18F-FDG in patients with progressive, metastatic prostate cancer. J Nucl Med. 2004;45(3):366–73.
64. Bonasera TA, O'Neil JP, Xu M, Dobkin JA, Cutler PD, Lich LL, et al. Preclinical evaluation of fluorine-18-labeled androgen receptor ligands in baboons. J Nucl Med. 1996;37(6):1009–15.
65. Silva RC, Sasse AD, Matheus WE, Ferreira U. Magnetic resonance image in the diagnosis and evaluation of extra-prostatic extension and involvement of seminal vesicles of prostate cancer: a systematic review of literature and meta-analysis. Int Braz J Urol. 2013;39(2):155–66.
66. Wibmer AG, Vargas HA, Hricak H. Role of MRI in the diagnosis and management of prostate cancer. Future Oncol. 2015;11(20):2757–66.
67. Vargas HA, Hotker AM, Goldman DA, Moskowitz CS, Gondo T, Matsumoto K, et al. Updated prostate imaging reporting and data system (PIRADS v2) recommendations for the detection of clinically significant prostate cancer using multiparametric MRI: critical evaluation using whole-mount pathology as standard of reference. Eur Radiol. 2016;26(6):1606–12.
68. von Below C, Daouacher G, Wassberg C, Grzegorek R, Gestblom C, Sorensen J, et al. Validation of 3 T MRI including diffusion-weighted imaging for nodal staging of newly diagnosed intermediate- and high-risk prostate cancer. Clin Radiol. 2016;71(4):328–34.
69. Turkbey B, Mena E, Shih J, Pinto PA, Merino MJ, Lindenberg ML, et al. Localized prostate cancer detection with 18F FACBC PET/CT: comparison with MR imaging and histopathologic analysis. Radiology. 2014;270(3):849–56.
70. Poulsen MH, Bouchelouche K, Hoilund-Carlsen PF, Petersen H, Gerke O, Steffansen SI, et al. [18F]fluoromethylcholine (FCH) positron emission tomography/computed tomography (PET/CT) for lymph node staging of prostate cancer: a prospective study of 210 patients. BJU Int. 2012;110(11):1666–71.
71. Beheshti M, Imamovic L, Broinger G, Vali R, Waldenberger P, Stoiber F, et al. 18F choline PET/CT in the preoperative staging of prostate cancer in patients with intermediate or high risk of extracapsular disease: a prospective study of 130 patients. Radiology. 2010;254(3):925–33.
72. Selnaes KM, Kruger-Stokke B, Elschot M, Willoch F, Storkersen O, Sandsmark E, et al. (18) F-Fluciclovine PET/MRI for preoperative lymph node staging in high-risk prostate cancer patients. Eur Radiol. 2018;28(8):3151–9.
73. Evangelista L, Guttilla A, Zattoni F, Muzzio PC, Zattoni F. Utility of choline positron emission tomography/computed tomography for lymph node involvement identification in intermediate- to high-risk prostate cancer: a systematic literature review and meta-analysis. Eur Urol. 2013;63(6):1040–8.

74. United States Food & Drug Administration. FDA Approves First PSMA-Targeted PET Imaging Drug for Men with Prostate Cancer; 2020. Available from: https://www.fda.gov/news-events/press-announcements/fda-approves-first-psma-targeted-pet-imaging-drug-men-prostate-cancer.
75. United States Food & Drug Administration. FDA approves second PSMA-targeted PET imaging drug for men with prostate cancer; 2021. Available from: https://www.fda.gov/drugs/drug-safety-and-availability/fda-approves-second-psma-targeted-pet-imaging-drug-men-prostate-cancer.
76. Pienta KJ, Gorin MA, Rowe SP, Carroll PR, Pouliot F, Probst S, et al. A phase 2/3 prospective multicenter study of the diagnostic accuracy of prostate-specific membrane antigen PET/CT with (18)F-DCFPyL in prostate cancer patients (OSPREY). J Urol. 2021:101097JU0000000000001698.
77. Hope TA, Armstrong WR, Murthy V, Heath CL, Behr S, Barbato F, et al. Accuracy of 68Ga-PSMA-11 for pelvic nodal metastasis detection prior to radical prostatectomy and pelvic lymph node dissection: a multicenter prospective phase III imaging study. J Clin Oncol. 2020;38(15_suppl):5502.
78. Hofman MS, Lawrentschuk N, Francis RJ, Tang C, Vela I, Thomas P, et al. Prostate-specific membrane antigen PET-CT in patients with high-risk prostate cancer before curative-intent surgery or radiotherapy (proPSMA): a prospective, randomised, multicentre study. Lancet. 2020;395(10231):1208–16.
79. Roach M 3rd, Hanks G, Thames H Jr, Schellhammer P, Shipley WU, Sokol GH, et al. Defining biochemical failure following radiotherapy with or without hormonal therapy in men with clinically localized prostate cancer: recommendations of the RTOG-ASTRO Phoenix Consensus Conference. Int J Radiat Oncol Biol Phys. 2006;65(4):965–74.
80. Han M, Partin AW, Pound CR, Epstein JI, Walsh PC. Long-term biochemical disease-free and cancer-specific survival following anatomic radical retropubic prostatectomy. The 15-year Johns Hopkins experience. Urol Clin North Am. 2001;28(3):555–65.
81. Hull GW, Rabbani F, Abbas F, Wheeler TM, Kattan MW, Scardino PT. Cancer control with radical prostatectomy alone in 1,000 consecutive patients. J Urol. 2002;167(2 Pt 1):528–34.
82. Freedland SJ, Humphreys EB, Mangold LA, Eisenberger M, Dorey FJ, Walsh PC, et al. Risk of prostate cancer-specific mortality following biochemical recurrence after radical prostatectomy. JAMA. 2005;294(4):433–9.
83. Kupelian PA, Mahadevan A, Reddy CA, Reuther AM, Klein EA. Use of different definitions of biochemical failure after external beam radiotherapy changes conclusions about relative treatment efficacy for localized prostate cancer. Urology. 2006;68(3):593–8.
84. Parker CC, Clarke NW, Cook AD, Kynaston HG, Petersen PM, Catton C, et al. Timing of radiotherapy after radical prostatectomy (RADICALS-RT): a randomised, controlled phase 3 trial. Lancet. 2020;396(10260):1413–21.
85. Yossepowitch O, Briganti A, Eastham JA, Epstein J, Graefen M, Montironi R, et al. Positive surgical margins after radical prostatectomy: a systematic review and contemporary update. Eur Urol. 2014;65(2):303–13.
86. Lange PH, Ercole CJ, Lightner DJ, Fraley EE, Vessella R. The value of serum prostate specific antigen determinations before and after radical prostatectomy. J Urol. 1989;141(4):873–9.
87. Patel A, Dorey F, Franklin J, deKernion JB. Recurrence patterns after radical retropubic prostatectomy: clinical usefulness of prostate specific antigen doubling times and log slope prostate specific antigen. J Urol. 1997;158(4):1441–5.
88. Moschini M, Sharma V, Zattoni F, Quevedo JF, Davis BJ, Kwon E, et al. Natural history of clinical recurrence patterns of lymph node-positive prostate cancer after radical prostatectomy. Eur Urol. 2016;69(1):135–42.
89. Beresford MJ, Gillatt D, Benson RJ, Ajithkumar T. A systematic review of the role of imaging before salvage radiotherapy for post-prostatectomy biochemical recurrence. Clin Oncol (R Coll Radiol). 2010;22(1):46–55.

90. Gomez P, Manoharan M, Kim SS, Soloway MS. Radionuclide bone scintigraphy in patients with biochemical recurrence after radical prostatectomy: when is it indicated? BJU Int. 2004;94(3):299–302.
91. Dotan ZA, Bianco FJ Jr, Rabbani F, Eastham JA, Fearn P, Scher HI, et al. Pattern of prostate-specific antigen (PSA) failure dictates the probability of a positive bone scan in patients with an increasing PSA after radical prostatectomy. J Clin Oncol. 2005;23(9):1962–8.
92. Kane CJ, Amling CL, Johnstone PA, Pak N, Lance RS, Thrasher JB, et al. Limited value of bone scintigraphy and computed tomography in assessing biochemical failure after radical prostatectomy. Urology. 2003;61(3):607–11.
93. Johnstone PA, Tarman GJ, Riffenburgh R, Rohde DC, Puckett ML, Kane CJ. Yield of imaging and scintigraphy assessing biochemical failure in prostate cancer patients. Urol Oncol. 1997;3(4):108–12.
94. Mitchell CR, Lowe VJ, Rangel LJ, Hung JC, Kwon ED, Karnes RJ. Operational characteristics of (11)c-choline positron emission tomography/computerized tomography for prostate cancer with biochemical recurrence after initial treatment. J Urol. 2013;189(4):1308–13.
95. Giovacchini G, Picchio M, Coradeschi E, Bettinardi V, Gianolli L, Scattoni V, et al. Predictive factors of [(11)C]choline PET/CT in patients with biochemical failure after radical prostatectomy. Eur J Nucl Med Mol Imaging. 2010;37(2):301–9.
96. Michaud L, Touijer KA, Mauguen A, Zelefsky MJ, Morris MJ, Lyashschenko SK, et al. (11) C-choline PET/CT in recurrent prostate cancer: retrospective analysis in a large U.S. patient series. J Nucl Med. 2020;61(6):827–33.
97. Fanti S, Minozzi S, Castellucci P, Balduzzi S, Herrmann K, Krause BJ, et al. PET/CT with (11)C-choline for evaluation of prostate cancer patients with biochemical recurrence: meta-analysis and critical review of available data. Eur J Nucl Med Mol Imaging. 2016;43(1):55–69.
98. Schuster DM, Savir-Baruch B, Nieh PT, Master VA, Halkar RK, Rossi PJ, et al. Detection of recurrent prostate carcinoma with anti-1-amino-3-18F-fluorocyclobutane-1-carboxylic acid PET/CT and 111In-capromab pendetide SPECT/CT. Radiology. 2011;259(3):852–61.
99. Bach-Gansmo T, Nanni C, Nieh PT, Zanoni L, Bogsrud TV, Sletten H, et al. Multisite experience of the safety, detection rate and diagnostic performance of fluciclovine ((18)F) positron emission tomography/computerized tomography imaging in the staging of biochemically recurrent prostate cancer. J Urol. 2017;197(3 Pt 1):676–83.
100. Andriole GL, Kostakoglu L, Chau A, Duan F, Mahmood U, Mankoff DA, et al. The impact of positron emission tomography with 18F-fluciclovine on the treatment of biochemical recurrence of prostate cancer: results from the LOCATE trial. J Urol. 2019;201(2):322–31.
101. Kim SJ, Lee SW. The role of (18)F-fluciclovine PET in the management of prostate cancer: a systematic review and meta-analysis. Clin Radiol. 2019;74(11):886–92.
102. Jani AB, Schreibmann E, Goyal S, Halkar R, Hershatter B, Rossi PJ, et al. (18)F-fluciclovine-PET/CT imaging versus conventional imaging alone to guide postprostatectomy salvage radiotherapy for prostate cancer (EMPIRE-1): a single centre, open-label, phase 2/3 randomised controlled trial. Lancet. 2021;397(10288):1895–904.
103. Fendler WP, Calais J, Eiber M, Flavell RR, Mishoe A, Feng FY, et al. Assessment of 68Ga-PSMA-11 PET accuracy in localizing recurrent prostate cancer: a prospective single-arm clinical trial. JAMA Oncol. 2019;5(6):856–63.
104. Nanni C, Schiavina R, Brunocilla E, Boschi S, Borghesi M, Zanoni L, et al. 18F-Fluciclovine PET/CT for the detection of prostate cancer relapse: a comparison to 11C-choline PET/CT. Clin Nucl Med. 2015;40(8):e386–91.
105. Okudaira H, Oka S, Ono M, Nakanishi T, Schuster DM, Kobayashi M, et al. Accumulation of trans-1-amino-3-[(18)F]fluorocyclobutanecarboxylic acid in prostate cancer due to androgen-induced expression of amino acid transporters. Mol Imaging Biol. 2014;16(6):756–64.
106. Schuster DM, Nanni C, Fanti S. Evaluation of prostate cancer with radiolabeled amino acid analogs. J Nucl Med. 2016;57(Suppl 3):61S–6S.

107. Calais J, Ceci F, Eiber M, Hope TA, Hofman MS, Rischpler C, et al. (18)F-fluciclovine PET-CT and (68)Ga-PSMA-11 PET-CT in patients with early biochemical recurrence after prostatectomy: a prospective, single-centre, single-arm, comparative imaging trial. Lancet Oncol. 2019;20(9):1286–94.
108. Fendler WP, Weber M, Iravani A, Hofman MS, Calais J, Czernin J, et al. Prostate-specific membrane antigen ligand positron emission tomography in men with nonmetastatic castration-resistant prostate cancer. Clin Cancer Res. 2019;25(24):7448–54.
109. Minner S, Wittmer C, Graefen M, Salomon G, Steuber T, Haese A, et al. High level PSMA expression is associated with early PSA recurrence in surgically treated prostate cancer. Prostate. 2011;71(3):281–8.
110. Yaxley JW, Raveenthiran S, Nouhaud FX, Samaratunga H, Yaxley WJ, Coughlin G, et al. Risk of metastatic disease on (68) gallium-prostate-specific membrane antigen positron emission tomography/computed tomography scan for primary staging of 1253 men at the diagnosis of prostate cancer. BJU Int. 2019;124(3):401–7.
111. Maurer T, Gschwend JE, Rauscher I, Souvatzoglou M, Haller B, Weirich G, et al. Diagnostic efficacy of (68)gallium-PSMA positron emission tomography compared to conventional imaging for lymph node staging of 130 consecutive patients with intermediate to high risk prostate cancer. J Urol. 2016;195(5):1436–43.
112. Woythal N, Arsenic R, Kempkensteffen C, Miller K, Janssen JC, Huang K, et al. Immunohistochemical validation of PSMA expression measured by (68)Ga-PSMA PET/CT in primary prostate cancer. J Nucl Med. 2018;59(2):238–43.
113. Ferraro DA, Ruschoff JH, Muehlematter UJ, Kranzbuhler B, Muller J, Messerli M, et al. Immunohistochemical PSMA expression patterns of primary prostate cancer tissue are associated with the detection rate of biochemical recurrence with (68)Ga-PSMA-11-PET. Theranostics. 2020;10(14):6082–94.
114. Siegel DA, O'Neil ME, Richards TB, Dowling NF, Weir HK. Prostate cancer incidence and survival, by stage and race/ethnicity – United States, 2001–2017. MMWR Morb Mortal Wkly Rep. 2020;69(41):1473–80.
115. Pascale M, Azinwi CN, Marongiu B, Pesce G, Stoffel F, Roggero E. The outcome of prostate cancer patients treated with curative intent strongly depends on survival after metastatic progression. BMC Cancer. 2017;17(1):651.
116. Scher HI, Morris MJ, Stadler WM, Higano C, Basch E, Fizazi K, et al. Trial design and objectives for castration-resistant prostate cancer: updated recommendations from the prostate cancer clinical trials working group 3. J Clin Oncol. 2016;34(12):1402–18.
117. Rathkopf DE, Beer TM, Loriot Y, Higano CS, Armstrong AJ, Sternberg CN, et al. Radiographic progression-free survival as a clinically meaningful end point in metastatic castration-resistant prostate cancer: the PREVAIL randomized clinical trial. JAMA Oncol. 2018;4(5):694–701.
118. Morris MJ, Molina A, Small EJ, de Bono JS, Logothetis CJ, Fizazi K, et al. Radiographic progression-free survival as a response biomarker in metastatic castration-resistant prostate cancer: COU-AA-302 results. J Clin Oncol. 2015;33(12):1356–63.
119. Kluetz PG, Ning YM, Maher VE, Zhang L, Tang S, Ghosh D, et al. Abiraterone acetate in combination with prednisone for the treatment of patients with metastatic castration-resistant prostate cancer: U.S. Food and Drug Administration drug approval summary. Clin Cancer Res. 2013;19(24):6650–6.
120. Weisman AJ, Harmon SA, Perk TG, Eickhoff J, Choyke PL, Kurdziel KA, et al. Quantification of bone flare on (18)F-NaF PET/CT in metastatic castration-resistant prostate cancer. Prostate Cancer Prostatic Dis. 2019;22(2):324–30.
121. Harmon SA, Perk T, Lin C, Eickhoff J, Choyke PL, Dahut WL, et al. Quantitative assessment of early [(18)F]sodium fluoride positron emission tomography/computed tomography response to treatment in men with metastatic prostate cancer to bone. J Clin Oncol. 2017;35(24):2829–37.

122. Beltran H, Tomlins S, Aparicio A, Arora V, Rickman D, Ayala G, et al. Aggressive variants of castration-resistant prostate cancer. Clin Cancer Res. 2014;20(11):2846–50.
123. Beltran H, Wyatt AW, Chedgy E, Donoghue A, Annala M, Warner E, et al. Impact of therapy on genomics and transcriptomics in high-risk prostate cancer treated with neoadjuvant docetaxel and androgen deprivation therapy. Clin Cancer Res. 2017.
124. Beltran H, Prandi D, Mosquera JM, Benelli M, Puca L, Cyrta J, et al. Divergent clonal evolution of castration-resistant neuroendocrine prostate cancer. Nat Med. 2016;22(3):298–305.
125. Dardenne E, Beltran H, Benelli M, Gayvert K, Berger A, Puca L, et al. N-Myc induces an EZH2-mediated transcriptional program driving neuroendocrine prostate cancer. Cancer Cell. 2016;30(4):563–77.
126. Mu P, Zhang Z, Benelli M, Karthaus WR, Hoover E, Chen CC, et al. SOX2 promotes lineage plasticity and antiandrogen resistance in TP53- and RB1-deficient prostate cancer. Science. 2017;355(6320):84–8.
127. Spratt DE, Gavane S, Tarlinton L, Fareedy SB, Doran MG, Zelefsky MJ, et al. Utility of FDG-PET in clinical neuroendocrine prostate cancer. Prostate. 2014;74(11):1153–9.
128. Fox JJ, Autran-Blanc E, Morris MJ, Gavane S, Nehmeh S, Van Nuffel A, et al. Practical approach for comparative analysis of multilesion molecular imaging using a semiautomated program for PET/CT. J Nucl Med. 2011;52(11):1727–32.
129. Rathkopf DE, Morris MJ, Fox JJ, Danila DC, Slovin SF, Hager JH, et al. Phase I study of ARN-509, a novel antiandrogen, in the treatment of castration-resistant prostate cancer. J Clin Oncol. 2013;31(28):3525–30.
130. Scher HI, Beer TM, Higano CS, Anand A, Taplin ME, Efstathiou E, et al. Antitumour activity of MDV3100 in castration-resistant prostate cancer: a phase 1–2 study. Lancet. 2010;375(9724):1437–46.
131. Morris MJ, Rowe SP, Gorin MA, Saperstein L, Pouliot F, Josephson D, et al. Diagnostic performance of (18)F-DCFPyL-PET/CT in men with biochemically recurrent prostate cancer: results from the CONDOR phase III, multicenter study. Clin Cancer Res. 2021.